ELSEVIER

18 February 1994

Chemical Physics Letters 218 (1994) 295–303

CHEMICAL PHYSICS LETTERS

Gas-phase infrared emission spectra of C_{60} and C_{70}. Temperature-dependent studies

Laszlo Nemes [a,1], Ram S. Ram [a,2], Peter F. Bernath [a,2], Frank A. Tinker [b], Michael C. Zumwalt [b], Lowell D. Lamb [b], Donald R. Huffman [b]

[a] *Department of Chemistry, University of Waterloo, Waterloo, Ontario, Canada N2L 3G1*
[b] *Department of Physics, University of Arizona, Tucson, Arizona, AZ 85721, USA*

Received 27 September 1993; in final form 9 December 1993

Abstract

The gas-phase infrared emission spectra of C_{60} and C_{70} were recorded by Fourier-transform spectroscopy. The measurements were carried out in the temperature range 500–950°C and the band positions were extrapolated to 0 K. In addition to the strong fundamental bands, numerous weak features were observed. We attribute these weak bands primarily to binary combination bands. Our measurements should prove useful for astronomical searches, low-temperature laboratory measurements and for detailed force-field calculations.

1. Introduction

Ever since the highly symmetric carbon clusters were discovered [1] and macroscopically produced [2], their existence in the interstellar medium and in the spectra of carbon-rich stars is an intriguing possibility [3]. For their detection in these astronomical sources, infrared observations should be based on gas-phase spectral data.

There have been intense experimental efforts to locate the allowed vibrational transitions of fullerenes, in particular for C_{60} and C_{70} [4–7]. Pressure- and temperature-dependent studies have been reported for the solid state [8–10]. Theoretical calculations were carried out to predict the full vibrational spectrum, including infrared and Raman active modes, as well as the forbidden modes [11–23]. For the inactive modes, inelastic neutron-scattering data are also available [24–26]. The theory for the vibration–rotation band structure, including complete symmetry classification, vibration–rotation interactions, and nuclear spin-statistics has been considered [27–31].

Gas-phase infrared spectral data were reported by some of the present authors [32] for C_{60}. In the present work we extend these previous studies to the determination of the temperature dependence of the C_{60} and C_{70} infrared emission bands. For C_{70} this work provides the first gas-phase experimental infrared data.

2. Experimental

The C_{60} and C_{70} samples used in this work were extracted from soot made by the standard arc evaporation procedure [2]. The C_{60} sample was prepared

[1] On leave from the Research Laboratory for Inorganic Chemistry, Hungarian Academy of Sciences, Budaorsi ut 45, Pf. 132, 1502 Budapest, Hungary.
[2] Also at: Department of Chemistry, University of Arizona, Tucson, Arizona, AZ 85721, USA.

SSDI 0009-2614(93)E1488-3

by flash chromatography of mixed fullerenes on an activated charcoal/silica column, using toluene as an eluent [33]. The purity of the C_{60} thus obtained was 99+% as measured by HPLC and UV–visible absorption spectroscopy, and the sample mass was ≈ 1 g. The C_{70} sample was obtained via chromatograph separation of mixed fullerenes using an alumina/hexane protocol [34,35]. The resulting C_{70} sample mass was ≈ 0.35 g, and the purity was 97+%, as determined by HPLC and UV–visible analysis.

Infrared emission spectra were recorded with the National Solar Observatory Fourier-transform spectrometer at the McMath Solar Telescope at Kitt Peak, Arizona. Two different spectral filters were used, an InSb filter between 480 and 1600 cm^{-1}, and an InAs filter between 480 and 2600 cm^{-1}. The lower wavenumber limit was set in both cases by the detector response and the beamsplitter transmission. Unapodized resolution was 0.10 cm^{-1} for C_{60} and 0.17 cm^{-1} for C_{70} with liquid helium cooled As:Si detectors and a KCl beamsplitter. Spectra were recorded as the samples were heated and each spectrum covered a temperature range of about 20°C. For C_{60}, 30 scans were co-added in 22 min of integration, while for C_{70} 50 scans were co-added in 20 min. The experimental procedures were similar to the previous measurements on C_{60} [32]. The temperature range for the series C_{60} spectra was 470–950°C, and 536–964°C for C_{70}. Background spectra of the furnace were also taken before heating to identify features not belonging to the fullerenes.

3. Symmetry and the vibrational partition function

The C_{60} molecule has icosahedral symmetry (I_h) and has 46 vibrational frequencies whereas the C_{70} molecule is of D_{5h} symmetry with 122 vibrational frequencies. For both molecules the vibrational partition function at room temperature is expected to be large because of the great number of modes, including many with low vibrational frequencies. Within the harmonic oscillator model, the vibrational partition function is given by the product [36]

$$Q_{\mathrm{vib}} = \prod_i \{g_i[1-\exp(-E_i/kT)]^{-1}\}, \qquad (1)$$

where g_i is the degeneracy of the ith mode. We have carried out a calculation of Q_{vib} for C_{60}, using reported infrared and Raman frequencies [4–7,32], and a compilation of optically "silent" modes, estimated theoretically and/or measured by inelastic neutron scattering [11–26]. On going from room temperature (300 K) to 800 K, the partition function increases from $\approx 10^3$ to $\approx 10^{22}$. We have not attempted a similar calculation for C_{70} but analogous results are expected. For C_{60}, between 300 and 800 K, the magnitude of Q_{vib} is well approximated by a simple empirical logarithmic formula

$$\log Q_{\mathrm{vib}} = -7.65 + 0.0367T. \qquad (2)$$

At the temperature of the emission spectra, the population of the vibrational ground state is very small indeed, and the probability of finding a C_{60} molecule in the zero-point state is about 10^{-21} at 773 K and about 10^{-38} at 1223 K. The expected vibrational composition of the infrared emission bands is then very complex, since vibrational anharmonicity allows transitions to change more than one quantum, and transitions from the numerous vibrationally excited levels are dominant. Although the population in any one excited vibrational level is small, the large number of such levels drains the population from the zero-point level.

Due to the center of symmetry in C_{60} and the high symmetry of C_{70} there are some restrictions on the possible infrared transitions. For example, first overtones ($v=2\leftrightarrow 0$) are forbidden for both clusters. Nevertheless, symmetry-allowed combination bands are very numerous. For example if transitions from the vibrational ground state to binary combinations of vibrational modes are considered then 380 combination bands are possible for C_{60} and 3568 for C_{70}.

4. Frequency and half-width of infrared emission bands

Peak frequency and bandwidth values (full width at half height) were extracted from the emission spectra by means of a spectral decomposition program (PC-DECOMP) written by Brault of the National Solar Observatory. The program uses Voigt profiles to fit spectra features. Due to the excessive "noisiness' in some spectral regions caused by sharp emission and absorption lines of small molecules like

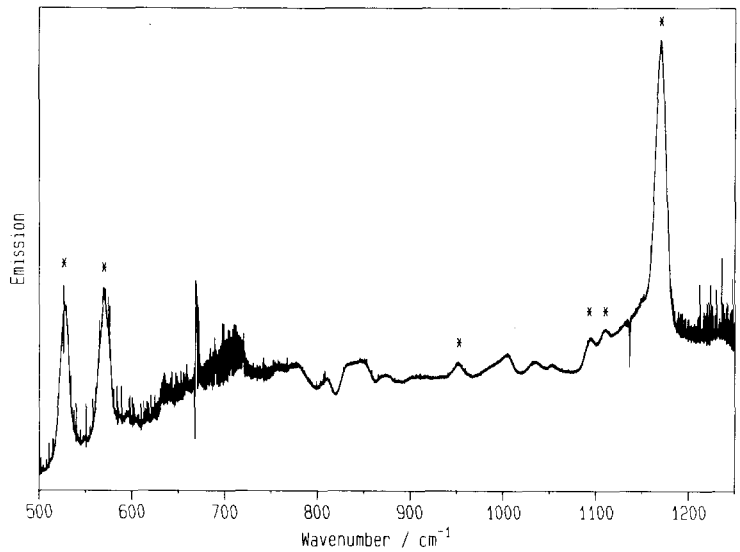

Fig. 1. The infrared emission spectrum of C_{60} (500–1250 cm^{-1}) with the C_{60} features marked with asterisks. The sharp features are due to impurity absorption and emission lines of small molecules.

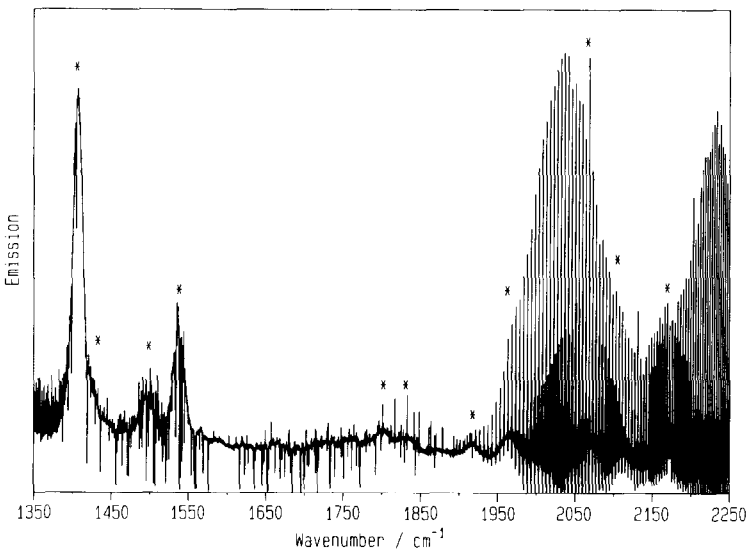

Fig. 2. The infrared emission spectrum of C_{60} (1350–2250 cm^{-1}) with the C_{60} features marked with asterisks.

CO_2 (Figs. 1–4), occasional hand measurements were also necessary. The accuracy of peak wavenumbers is generally better than one cm^{-1}, while the bandwidth values are less accurate as discussed below. The observed band positions are reported in Tables 1 and 2, while Tables 3 and 4 contain peak positions and widths extrapolated to 0 K. The 0 K line positions may be useful for astronomical searches and for low temperature, gas-phase laboratory measurements.

Peak frequencies decrease with increasing temperature, whereas bandwidths increase. There are two main sources for these temperature effects: the role of "hot" vibrational transitions and the change in the rotational structure of the bands. With increasing temperature the population of excited vibrational levels leads to red-shifts in the peak frequency be-

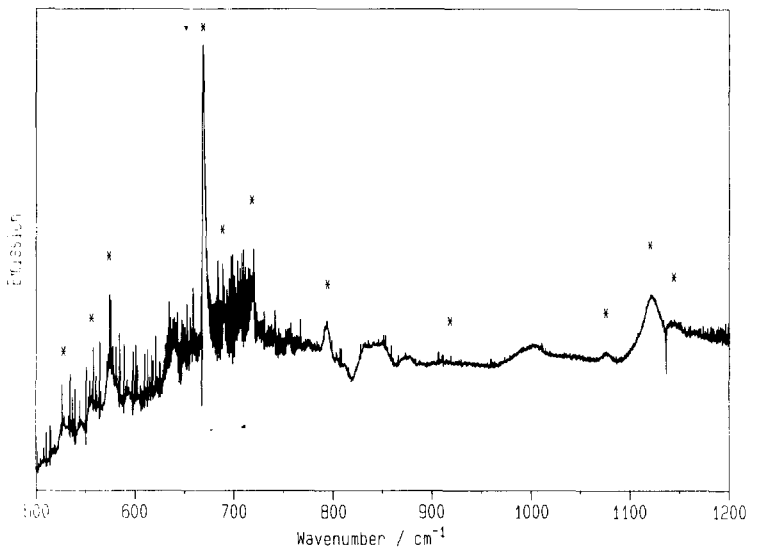

Fig. 3. The infrared emission spectrum of C_{70} (500–1200 cm^{-1}) with the C_{70} features marked with asterisks.

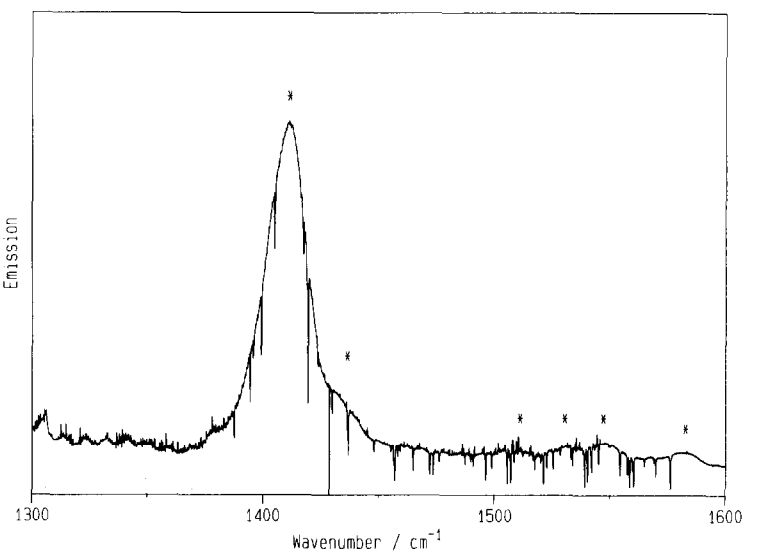

Fig. 4. The infrared emission spectrum of C_{70} (1300–1600 cm^{-1}) with the C_{70} features marked with asterisks.

cause anharmonicity causes hot bands to appear at the low-frequency side of fundamentals. In addition each vibrational transition has a superimposed rotational envelope that broadens with increasing temperature. The "true" peak frequency was obtained by linearly extrapolating the data reported in Tables 1 and 2 to absolute zero as reported in Tables 3 and 4.

The extrapolation of bandwidth values ($\Delta\nu$) to absolute zero was carried out by using the function

$$\Delta\nu = aT^{1/2} + bT. \tag{3}$$

A dependence on the square root of T is expected based on the theoretical work of Weeks and Harter [29], and indeed in most cases when the widths are plotted against $T^{1/2}$ good linearity is observed in the range of our temperatures. However, such a plot results in physically unreasonable extrapolated widths (they come out as negative quantities), while one ex-

Table 1
Temperature-dependent wavenumbers and widths for the fundamental vibrations of C_{60} (cm^{-1})

Temperature (K)	ν_{25}	ν_{26}	ν_{27}	ν_{28}
879	1412.9	–	–	–
905	1412.1	–	–	–
925	1412.0 (12.4) [a]	–	–	–
941	1411.5 (12.6)	–	–	–
951	–	1171.0 (13.4) [b]	570.4	528.2 (10.0) [a]
960	1409.0	1173.0	–	–
1049	–	1165.6	570.1 (13.3) [a]	527.5
1066	1407.2 (13.5)	–	–	–
1083	–	1165.8	570.0 (13.7)	527.5 (11.6)
1110	1408.3 (14.3)	1170.2	–	–
1141	–	1168.6	569.7 (13.5)	527.5 (11.5)
1177	1404.3	1166.4	–	–
1212	–	1167.3	569.4 (14.1)	–

[a] The full width at half maximum is in parentheses.
[b] The average width is given over the entire temperature range.

Table 2
Temperature-dependent wavenumbers and widths for the strong vibrational modes of C_{70} (cm^{-1})

Temperature (K)	ν_{24}	ν_{30}	ν_{33}	ν_{36}	ν_{37}	ν_{38}	ν_{79}	ν_{82}
929	–	1126.0	793.3 (7.3) [a]	638.5 (10.6) [a]	–	–	–	–
965	1413.6 (17.1) [b]	–	–	–	–	–	–	–
998	–	1124.5	–	–	575.5 (8.9) [a]	557.8	–	530.3
1011	1412.7 (17.8)	–	–	–	576.3	557.1	–	528.7
1028	– (17.8)	–	–	–	–	–	–	–
1043	–	1122.7 (13.6) [b]	–	–	575.7	557.6	1077.3	528.8 (10.0)
1071	1411.8 (18.2)	1121.5	–	–	–	–	–	–
1074	–	–	–	–	575.1	556.3	–	529.5
1099	–	1121.7 (14.7)	–	–	574.9	556.9	1077.0	527.6 (10.0)
1124	1410.5	–	–	–	–	–	–	–
1151	–	1121.6 (17.5)	–	–	575.5	556.5	1075.6	527.5
1174	– (22.6)	–	–	–	–	–	–	–
1199	–	1120.5 (18.6)	–	–	574.7	555.5	1074.3	526.2 (10.0)
1222	– (23.2)	–	–	–	–	–	–	–
1233	–	1115.5 (21.1)	–	–	574.1	–	–	526.4

[a] The full width at half maximum is in parentheses.
[b] The average position and width over the observed temperature range.

Table 3
Temperature dependence of peak positions and widths for C_{60}

Fundamental	Peak frequency		Band-width coeff.		Temp. range (°C)
	position (0 K) (cm^{-1})	slope (cm^{-1}/K)	a ($cm^{-1} K^{-1/2}$)	b ($cm^{-1} K^{-1}$)	
$\nu_{25}(t_{1u})$	1435.53 (1.03) [a]	−0.0260 (36)	0.246 (69)	0.0053 (22)	607–905
$\nu_{26}(t_{1u})$	1190.75 (97)	−0.0196 (39)			607–905
$\nu_{27}(t_{1u})$	574.37 (6)	−0.0041 (3)	0.517 (47)	−0.0032 (14)	653–905
$\nu_{28}(t_{1u})$	531.22 (24)	−0.0033 (18)			607–939

[a] One standard deviation error in parentheses.

Table 4
Temperature dependence of peak positions and widths for C_{70}

Fundamental	Peak frequency		Temp range (°C)
	position (0 K) (cm^{-1})	slope (cm^{-1}/K)	
$\nu_{24}(e_1')$	1431.977 (19) [a]	−0.0190 (10)	624–949
$\nu_{30}(e_1')$	1144.06 (54)	−0.0200 (20)	656–960
$\nu_{33}(e_1')$	793.34 (58) [b]	–	726–925
$\nu_{36}(e_1')$	638.47 (87) [b]	–	777–961
$\nu_{37}(e_1')$	583.14 (38)	−0.0071 (17)	726–961
$\nu_{38}(e_1')$	567.67 (34)	−0.0099 (19)	726–926
$\nu_{79}(a_2'')$	1099.55 (43)	−0.0209 (39)	777–926
$\nu_{82}(a_2'')$	545.02 (65)	−0.0153 (28)	726–926

[a] One standard deviation error in parentheses.
[b] The average over the observe temperature range.

Table 5
Comparison of infrared spectral data for the C_{60} fundamentals (cm^{-1})

Mode	Gas phase			Solid state		Argon matrix [d]
	0 K [a]	1083 K [a]	1065 K [b]	300 K	15 K [d]	
$\nu_{25}(t_{1u})$	1435.5	1407.2 [e]	1406.9	1429.8	1432.3 [f]	1431.8
$\nu_{26}(t_{1u})$	1190.8	1165.8	1169.1	1183.0	1183.7	1184.8
$\nu_{27}(t_{1u})$	574.4	570.0	570.3	576.1	576.5	579.3
$\nu_{28}(t_{1u})$	531.2	527.5	527.1	526.2	525.2	530.1

[a] This work. [b] Ref. [32]. [c] Ref. [10].
[d] Ref. [37]. [e] 1066 K. [f] Highest frequency component.

Table 6
Comparison of infrared spectral data for the C_{70} fundamentals (cm^{-1})

Mode	Gas phase at 0 K [a]	IR emission at 1071 K [a]	Solid state		
			ref. [6]	ref. [7]	ref. [10]
$\nu_{24}(e_1')$	1432.0	1411.8	1430.0	1431.0	1430.9
$\nu_{30}(e_1')$	1144.1	1122.2	1134.0	1134.0	1132.9
$\nu_{33}(e_1')$	(793) [b]	793.3	795.0	799.0	795.4
$\nu_{36}(e_1')$	(638) [b]	638.5	642.0	642.0	642.5
$\nu_{37}(e_1')$	583.1	575.3	578.0	579.0	577.6
$\nu_{38}(e_1')$	567.7	553.3	565.0	565.0	566.2
$\nu_{79}(a_2'')$	1099.6	1077.2	1086.0	–	–
$\nu_{82}(a_2'')$	545.0	528.2	535.0	535.0	534.6

[a] This work. [b] Average over the observed temperature range.

pects zero width at $T=0$ K. Therefore the empirical equation (3) was used. Tables 3 and 4 contain the coefficients of these two variable regressions. Note that for C_{70} and for two of the four fundamentals of C_{60}, the bandwidth data were not good enough to give a reasonable fit using Eq. (3). Previous studies on the temperature dependence of vibrational spectra of these fullerenes [9,10] were carried out in the solid state at temperatures below 350 K.

It is interesting to compare our extrapolated peak

frequencies to the results of argon matrix isolation studies and solid state measurements of C_{60} (Table 5) and C_{70} (Table 6). The 0 K extrapolated frequency values for C_{60} are very similar to the matrix values, except for ν_{26} and ν_{27} where there are 5–6 cm^{-1} differences. The argon matrix shifts are remarkably small. The room-temperature solid state line positions are also quite close to the extrapolated 0 K positions for both C_{60} and C_{70} (Tables 5 and 6).

5. Assignment of the spectral features

The fundamentals of C_{60} were reported in the previous gas-phase work at a temperature of 1065 K. In the present spectra the signal-to-noise ratio is much better than earlier. For the C_{70} molecule our measurements constitute the first gas-phase values in the literature. The C_{70} molecule has 31 infrared-active frequencies ($21\,e_1' + 10\,a_2''$) [#1], out of which we could assign eight stronger ones, not masked in our spectra by other features. The assignments were based on the available solid state work [6,7,10] and theoretical calculations [14,16,18,19]. The identified bands are collected in Table 6 and comparisons are also given to previous solid state work. The solid state spectra were taken at room temperature. There is a medium strong band of C_{70} near 674 cm^{-1} in the solid state ($\nu_{81}(a_2'')$) but it is overlapped by impurity CO_2 emission in our spectra. All of our emission bands have a lower wavenumber than in the solid state [6,7,10]. The greatest difference is found for the strong emission band at about 1412 cm^{-1} that, on intensity grounds, must correspond to the strong feature at 1430 cm^{-1} in the solid state ($\nu_{24}(e_1')$). The band at 1414 cm^{-1} in solid C_{70} has a much lower intensity (see refs. [6,7,10]) and we have no evidence for it in the emission spectra (apart from a very weak feature around 1380 cm^{-1}). Another assignment difficulty is that of ν_{79} at 1077 cm^{-1} in our high-temperature spectra. The corresponding solid state feature was only reported by Bethune et al. [6] as an uncertain assignment for a weak band. Since it is a significant feature in our spectra we assume it to be a fundamental.

There are many weaker features in both C_{60} and C_{70} emission spectra, some of which are listed in Table 7. Such features have been reported from solid state measurements [10], some of which are also listed in Table 7. We are able to find corresponding solid state features in the work of Chase et al. [10]. To account for these weak bands one has several alternatives. The first possible explanation is that they belong to impurities, such as smaller or larger fullerene clusters and solvents. The second possibility (for the solid state work) is that they are caused by solid state effects, but this is, of course, not possible for our gas-phase spectra. The third explanation is that these bands are due to singly ^{13}C-substituted C_{60} and C_{70} molecules, due to the natural abundance of the ^{13}C nucleus. Finally these modes might be combination bands. (As we discussed earlier first overtones are symmetry forbidden in both molecules.)

We have looked for C_{70} features in the C_{60} spectra and vice versa. The results were negative with the interesting case of ν_{25} for C_{60} and ν_{24} for C_{70}. These bands have practically identical positions in the emission spectra, and even their extrapolated frequencies are very similar, as can be seen from Tables 3 and 4. However there is no feature at 1169 cm^{-1} in the C_{70} spectra that would be diagnostic for the presence of C_{60}. In view of the purity of our samples, we

Table 7
Weak features in the C_{60} and C_{70} emission spectra (cm^{-1})

C_{60}		C_{70}
this work	ref. [10]	this work
951	962.8	706
1035	1038.5	716
1094	1100.2	950
1110	1115.1	1166
1425	1430.0	1190
1497	1502.8	1510
1538	1538.9	1530
1800	1817.1	1546
1833	1852.8	1581
1919	1936.2	
1967	1989.2	
2065	2076.5	
2110	2121.3	
2170	2191.2	

[#1] The numbering system we use for the fundamentals follows the usual Mulliken convention. For C_{60} it adheres to that of Brensdal et al. [13], while for C_{70} the order is given by the group structure: $12a_1' + 9a_2' + 21e_1' + 22e_2' + 9a_1'' + 10a_2'' + 19e_1'' + 20e_2''$.

rule out impurities as the cause of the features.

The probability of having one ^{12}C substituted by ^{13}C is 0.345 in C_{60} [31], so that there is a good chance of seeing $^{13}C^{12}C_{59}$ and $^{13}C^{12}C_{69}$ spectra. However a single carbon isotope substitution lowers the symmetry to C_s and all 174 modes in C_{60} become infrared active. The oscillator strength of the allowed modes in C_{60} becomes distributed among many modes in $^{13}C^{12}C_{59}$. Also each triply degenerate mode splits to two in-plane modes and one out-of-plane mode. However, the mass effects are weak and we expect the ^{13}C-substituted molecule to possess its strongest fundamentals in the neighborhood of the t_{1u} modes in $^{12}C_{60}$. This isotopic perturbation was examined by Weeks [38] who found that a single ^{13}C substitution splits the t_{1u} modes by an amount between 0.5 and 2.0 cm^{-1}. It seems unlikely that isotopic effects can account for the many weak bands.

Thus we are left with non-fundamental vibrational transitions as the cause of the weak features. As we have discussed earlier, there is a great number of binary combinations that should be considered first. Most of the combination bands involve infrared silent modes, for which there are no accurate frequency estimates. For C_{60} some of the combination bands, those between known Raman-active modes and the t_{1u} infrared-active ones ($t_{1u}\otimes a_g$, $t_{1u}\otimes h_g$), can be predicted reliably. Anharmonic red-shifts were found small (between 0.06 and 0.67 cm^{-1} for the t_{1u} fundamentals) by Weeks [38], so that we may expect the combination tones to be fairly close to the sum of the t_{1u} and a_g, or t_{1u} and h_g mode frequencies. Using experimental values we can find only three tentative assignments: $\nu_{25}(t_{1u})+\nu_{20}(h_g)=1407+772=2179$ cm^{-1}, $\nu_{25}(t_{1u})+\nu_{12}(h_g)=1407+711=2118$ cm^{-1}, and $\nu_{25}(t_{1u})+\nu_{22}(h_g)=1407+429=1836$ cm^{-1}. These values are close to three weak features (2170, 2210 and 1833 cm^{-1}) in the C_{60} spectra (see Table 7).

Using estimated values for the silent modes we have tried to simulate the 380 binary combinations for C_{60} and about half of the 3568 combinations (below 1900 cm^{-1}) for C_{70}. A frequency histogram that assumes that all transitions have the same intensity leads to the prediction of considerable combination tone intensity in the wavenumber range 1700–2200 cm^{-1} for C_{60} and a steadily increasing intensity from 500 to 1900 cm^{-1} for C_{70}. Indeed most of the features in Table 7 occur in these regions. Such simple considerations are, however, very naive. Detailed force field calculations (preferably anharmonic) are required to assign all of the features that we see.

6. Acknowledgement

The National Optical Astronomy Observatories is operated by the Association of Universities for Research in Astronomy, Inc., under contract with the National Science Foundation. We thank J. Wagner for assistance in operating the spectrometer. Support for PFB and RSR and for DRH was provided by grants from the NASA Origins of the Solar System Program. LN and PFB are grateful for funding from Natural Sciences and Engineering Research Council of Canada. LN thanks the Hungarian Research Fund (OTKA I/5; T007643) for support. Acknowledgement is made to the Petroleum Research Fund, administered by the American Chemical Society, for partial support of this work. Support for MCZ, FAT, LDL and DRH was provided by the Division of Advanced Energy Projects of the Office of Basic Energy Sciences, Department of Energy. We thank B. Chase for providing the weak C_{60} band positions quoted in Table 7.

7. References

[1] H.W. Kroto, J.R. Heath, S.C. O'Brien, R.F. Curl and R.E. Smalley, Nature 318 (1985) 162.
[2] W. Krätschmer, L.D. Lamb, K. Fostiropoulos and D.R. Huffman, Nature 347 (1990) 354.
[3] H.W. Kroto and M. Jura, Astron. Atrophys. 263 (1992) 275.
[4] D.S. Bethune, G. Meijer, W.C. Tang and H.J. Rosen, Chem. Phys. Letters 174 (1990) 21.
[5] T.J. Dennis, J.P. Hare, H.W. Kroto, R. Taylor, D.R.M. Walton and P.J. Hendra, Spectrochim. Acta 47 A (1991) 1289.
[6] D.S. Bethune, G. Meijer, W.C. Tang, H.J. Rosen, W.G. Golden, H. Seki, C.A. Brown and M.S. de Vries, Chem. Phys. Letters 179 (1991) 181.
[7] R.A. Jishi, M.S. Dresselhaus, G. Dresselhaus, K.A. Wang, P. Zhou, A.M. Rao and P.C. Eklund, Chem. Phys. Letters 206 (1993) 187.
[8] K. Aoki, H. Yamawaki, Y. Kakudate, M. Yoshida, S. Usuba, H. Yokoi, S. Fujiwara, Y. Bae, R. Malhotra and D. Lorents, J. Phys. Chem. 95 (1991) 9037.

[9] V.S. Babu and M.S. Seehra, Chem. Phys. Letters 196 (1992) 569.
[10] B. Chase, N. Herron and E. Holler, J. Phys. Chem. 96 (1992) 4262; private communication.
[11] Z.C. Wu, D.A. Jelski and T.F. George, Chem. Phys. Letters 137 (1987) 291.
[12] R.E. Stanton and M.D. Newton, J. Phys. Chem. 92 (1988) 2141.
[13] E. Brensdal, B.N. Cyvin, J. Brunvoll and S.J. Cyvin, Spectry. Letters 21 (1988) 313.
[14] F. Negri, G. Orlandi and F. Zerbetto, J. Am. Chem. Soc. 113 (1991) 6037.
[15] G.B. Adams, J.B. Page, O.F. Sankey, K. Sinha, J. Menendez and D.R. Huffman, Phys. Rev. B 44 (1991) 4052.
[16] K. Raghavachari and C.M. Rohlfing, J. Phys. Chem. 95 (1991) 5768.
[17] R.A. Jishi, R.M. Mirie and M.S. Dresselhaus, Phys. Rev. B 45 (1992) 13685.
[18] C.Z. Wang, C.T. Chan and K.M. Ho, Phys. Rev. B 46 (1992) 9761.
[19] P. Procacci, G. Cardini, P.R. Salvi and V. Schettino, Chem. Phys. Letters 195 (1992) 347.
[20] G. Dresselhaus, M.S. Dresselhaus and P.C. Eklund, Phys. Rev. B 45 (1992) 6923.
[21] H. Xia, Q. Jiang and D. Tian, Chem. Phys. Letters 198 (1992) 109.
[22] Q. Jiang, H. Xia, Z. Zhang and D. Tian, Chem. Phys. Letters 192 (1992) 93.
[23] G. Onida and G. Benedek, Europhys. Letters 18 (1992) 403.
[24] K. Prassides, T.J.S. Dennis, J.P. Hare, J. Tomkinson, H.W. Kroto, R. Taylor and D.R.M. Walton, Chem. Phys. Letters 187 (1991) 455.
[25] W.A. Kamitakahara, J.S. Lannin, R.L. Cappelletti, J.R.D. Copley and F. Li, Physica B 180/181 (1992) 709.
[26] C. Christides, A.V. Nikolaev, T.J.S. Dennis, K. Prassides, F. Negri, G. Orlandi and F. Zerbetto, J. Phys. Chem. 97 (1993) 3641.
[27] W.G. Harter and D.E. Weeks, Chem. Phys. Letters 132 (1986) 387.
[28] D.E. Weeks and W.G. Harter, J. Chem. Phys. 90 (1989) 4744.
[29] D.E. Weeks and W.G. Harter, Chem. Phys. Letters 176 (1991) 209.
[30] W.G. Harter and T.C. Reimer, J. Chem. Phys. 94 (1991) 5426.
[31] W.G. Harter and T.C. Reimer, Chem. Phys. Letters 194 (1992) 230.
[32] C.I. Frum, R. Engleman Jr., H.G. Hedderich, P.F. Bernath, L.D. Lamb and D.R. Huffman, Chem. Phys. Letters 176 (1991) 504.
[33] W.A. Scrivens, P.V. Bedworth and J.M. Tour, J. Am. Chem. Soc. 114 (1992) 7917.
[34] K. Chatterjee, D.A. Parker, P. Wurz, K.R. Lykke, D.M. Gruen and L.M. Stock, J. Org. Chem. 57 (1992) 3253.
[35] K.C. Khemani, M. Prato and F. Wudl, J. Org. Chem. 57 (1992) 3254.
[36] E.B. Wilson Jr., J.C. Decius and P.M. Cross, Molecular vibrations (McGraw-Hill, New York, 1955) Sections 7–9.
[37] R.E. Haufler, J. Conceicao, L.P.F. Chibante, Y. Chai, N.E. Byrne, S. Flanagan, M.M. Haley, S.C. O'Brien, C. Pan, Z. Xiao, W.E. Billups, M.A. Ciufolini, R.H. Hauge, J.L. Margrave, L.J. Wilson, R.F. Curl and R.E. Smalley, J. Phys. Chem. 94 (1990) 8634.
[38] D.E. Weeks, J. Chem. Phys. 96 (1992) 7380.